

Study and Evaluation of Parameters Influencing Parkinson's Disease Using 3D CNN

Caroline El Fiorenza J* and V. Sellam

SRM Institute of Science and Technology, Department of Computer Science and Engineering, Chennai, India

Received: 22 Apr. 2023, Revised: 22 May 2023, Accepted: 2 Jun. 2023

Published online: 1 Jul. 2023

Abstract: A diagnostic method of determining protein structure in persons for Parkinson's disease (PD) would be a 3D imaging scan. Convolutional Neural Networks (CNNs), which are efficient when used with spatial data, are suitable candidates for automating this diagnostic procedure to assist medical workers. The protein structure of PD patients was evaluated or diagnosed using an Improved Faster Recurrent Convolutional Neural Network (IFRCNN) ordinal model in this article. A data preprocessing technique was modified to operate PD because IFRCNNs require big datasets to operate acceptably. We take into account the Improved Shortest Paths Ordinal Graph-based Oversampling (ISP-OGO) technique that employs a gamma probabilistic model for the creation of Inter-Class Data (ICD). It is proposed that ISP-OGO be modified to become the ISP-OGO- β method that uses the beta distribution, which is more appropriate than gamma for creating synthetic samples in the ICD. A novel 3D image dataset is the foundation for the evaluation of the various approaches demonstrates how ISP-OGO- β produces greater performance than ISP-OGO and the ordinal method enhances the effectiveness compared to the nominal method.

Keywords: Parkinson's Disease, Spatial Data, Improved Faster Recurrent Convolutional Neural Network, Inter-Class Data Generation, Decision Support Systems, Improved Shortest Paths Ordinal Graph-based Oversampling

1 Introduction

PD was a chronic neurological condition that impacts motion and progresses over time. The proportion of PD rises with aging and is presently between 1 and 3% in people over 65 years of age making it the 2nd most common neurodegenerative condition after Alzheimer's Disease (AD) [1,2]. Although the disease's cause has not yet been identified, it is associated with the death of dopaminergic neurons, which results in fewer dopamine transporters in the striatum. In actuality, dopaminergic neurons in the substantia nigra create the neurotransmitter dopamine, which is then carried along the nigrostriatal route to the striatum and made up of the caudate and putamen [3]. Although there is currently no cure for PD, early identification enables efficient control to slow the rate of development and may aid in the creation of novel therapeutic approaches.

Tremor, rigidity, & gradualness of movement are the most prevalent and common side effects of idiopathic Parkinson's [4]. This type typically responds well to medications that increase or replace dopamine atoms in the brain. A rare form of parkinsonism called corticobasal

degeneration affects people starting at age 40, typically between the ages of 50 and 70. It usually starts out affecting one part of the body more than the other before gradually spreading over a few years. Progressive Supranuclear Palsy (PSP) and Cortico Basal Degeneration (CBD) are similar [5]. Some people with CBD later develop PSP and vice versa. 'Alien limb' disorder, which causes the arms or legs to appear to move autonomously, difficulty controlling the appendages on one side of the body, numbness & unfortunate facilitation of development in one hand, making routine tasks like dressing, eating difficult, shaking, writing, muscle rigidity, jerky or ungainly development and fits, adjust and coordination issues, etc. are some of the symptoms of CBD [6,7].

According to estimates, there are 120 to 180 PD sufferers for every 100,000 people, and the percentage is rising as people are living longer. Researchers have spent decades trying to learn more about this condition to properly restrict its symptoms, which are typically recurrent muscle rigidity and/or tremor. Later stages of PD may include additional symptoms such as dysarthria,

* Corresponding author e-mail: caro.fiorenza@gmail.com

akinesia & bradykinesia [8]. Expert systems & decision support systems have been developed recently in Artificial Intelligence (AI) for use in medical applications. Attempts to simulate Biological Neural Networks (BNN) what led to the development of Artificial Neural Network (ANN). When neurons are triggered, axons are used to transfer nerve impulses from one neuron to another. A neuron's dendrites, which are growths from the cell bodies of the neurons, connect it to the axons of other neurons [9]. Synapses are the points of contact between an axon or a dendrite. Our study's objective was to evaluate a Deep Learning method that uses cascaded 3D CNNs to predict and diagnose protein structures to detect less severe diseases at an earlier phase. Proteins of various shapes have been detected in the spinal fluid of Parkinson's sufferers and healthy people. To recognize the same and provide a handling model. To help Parkinson's patients, develop and test ML algorithms.

2 Related Work

PD diagnosis is one of the numerous clinical applications for Machine Learning (ML) that have been discussed in the literature. Shaking, slowness, trouble walking & abnormal gaits are the main motor signs of PD, a DNS condition that affects the brain. Some problems were connected to issues with sleep, emotion, or senses [10, 11]. While patient care and nursing home fees make up the largest portion of the cost of this condition, the cost to society increases as the symptoms get worse. The overall prize was predicted to £3.3 billion & £445 million a year in the UK [12]. A critical component of choosing the right treatment for PD patients is determining how severe their diagnosis is because an excessively high dose of levodopa may eventually make their symptoms worse [13].

Threshold models are another approach that is frequently employed to solve this issue. It is a presumption that there is an underlying latent continuous variable from which multiple ranks can be derived by setting various criteria [14]. The latent variable's value as well as the criteria must therefore be determined from the data in this approach. Certain strategies, like the traditional proportional odds approach and the current gologit method, fit the framework of the CLM, a statistical method for calculating the likelihood of clusters belonging to related groups while accounting for the ordinal scale [15]. Some ordinal methods involve breaking the ordinal issue down to a collection of binary issues. In certain cases, such as the cascade linear utility method [16], these decompositions are handled by a collection of various methods. In other instances, they are represented by a number of the same underlying model's outputs. A similar problem arises with all OBDs: integrating the outcomes of decomposition into a particular final categorization [17]. The earliest methods need the 1st class to pass a particular mark; however, this can cause an imbalance because it's harder to choose the

last classes [18]. Error Correcting Codes are more appropriate for this task since it taken into account all outputs equally while making a decision.

Through the use of existing data, ML techniques can automate some of these operations. To aid medical professionals in making a better decision or offering a second opinion, they might act as the central component of a decision support system [19]. Particularly in the clinic area where healthy patients were far more prevalent suffering ones, segmentation assignments could patient of unbalanced data. Moreover, data collection and accurate labeling are costly and time-consuming [20]. In this case, the performance of ML models needs to be improved by the use of data augmentation approaches [21]. The simplest method for enhancing spatial data, such as medical imaging, is to translate, rotate, flip, and crop the images. Depending on the particular job to be learned, a combination of these can be employed [22]. Cropped Areas of Interest could be utilized as samples to expedite object detection activities like lesion or abnormality detection. Low dimensional data are a good fit for age-old methods like Synthetic Minority Oversampling. Convolutional activities can be used by some methods, like Autoencoders, to enhance performance and efficiency for spatial data [23, 24]. Furthermore, to avoid traps like mode collapse, those methodologies call for a substantial amount of training examples.

The production of example the ICD of the hidden manifold was proposed to utilize a gamma distribution. Although this distribution favors the area of the graph closest to the class to be enhanced, it nevertheless allows for the inclusion of characteristics in the boundaries of groups. Furthermore, this has several drawbacks [25]. The production of values in a compact area is not suitable for the gamma distribution [26]. This is not just a theoretical oversight, but it also makes it difficult to meaningfully tune its settings, depending on the database to which it is implemented. This paper proposes a better-suited beta distribution as a replacement for the gamma distribution. This distribution allows for a higher degree of adaptability that could help to improve performance.

3 Proposed System

3.1 Data description

The Clinical Management Unit (CMU) of Nuclear Medicine (NM) at the Hospital Universitario "Reina Sofa" contributed 508 3D pictures to the database [27]. 314 photos are of healthy people, while 42 exhibit just minor changes, 52 show more significant changes and 100 reveal severe changes. These types of MD files usually suffer from a major imbalance problem. Less than 10% of the samples in our case are from class 1 patients, while more than 60% are from healthy persons. Each of the photos has a class designation that indicates the

doctors’ prognosis. The identification of which of the 4 groups an image falls into can be framed as an ordinal classification problem due to the progressive structure of these classes, and consequently, specialized strategies can be used to leverage the order information.

The foundation of our analytical technique is a cascaded 3D IFRCNN framework, which was a standard 3-layer stage of an ANN for final classification. $10 \times 130 \times 130$ voxels made up the original size of the volume of interest sent to ANN & CNN. Convolutional blocks alternate with pooling & dropout blocks in the IFRCNN model [28]. Convolutional frames apply a filter to pictures to extract the qualities required for classification. Blocks that use pooling take advantage of dimensional reduction. Last but not least, dropout blocks, which regularly remove neuronal clusters, are crucial in preventing overfitting during learning. The overall results, as depicted in Figure 1, are obtained by flattening the resulting tensor and applying it to 3 dense layers with a “softmax” activation algorithm.

The “back-propagation” procedure, which is used in the development of neural networks, is quite unusual and begins with a collection of parameters that are randomly allocated to control reaction to stimuli. The stimulus is then provided, the outcome was matched to the correct label, and parameters are then adjusted to improve the outcome’s precision. In the present instance, the network was fed with all of the chosen images and the so-called loss function, which measures classification error was then assessed [29]. The loss-function value should fall very frequently as accuracy rises in a great training cycle. Both the error and precision were evaluated on the training dataset and the verification dataset at every single step of the procedure. Both of the images’ trends serve as indicators of how well education is working.

3.2 Proposed ordinal classification

When the classes are arranged, OBD can be used to solve the problem by breaking it down into $Q - 1$ binary decision problems rather than tackling it as a whole, as was previously described. Every q-problem involves determining whether $y > C_q$ is conditioned to x . Naturally, It could necessitate $Q - 1$ different method, which could resolve one of these binary issues. This strategy, as initially proposed, would entail computing each likelihood $p_q = P(y = C_q)$ based on the gathered methods before choosing the category with maximum probability. The specific likelihood was calculated as an operation to the binary algorithms’ predicted cumulative likelihood ($y > C_q$).

$$p_1 = P(y = C_1) = 1 - P(y > C_1) \tag{1}$$

$$p_q = P(y = C_q) = P(y > C_{q-1}) - P(y > C_q) \forall 1 < q < Q \tag{2}$$

$$p_Q = P(y = C_1) = P(y > C_{Q-1}) \tag{3}$$

Unfortunately, this method has several drawbacks. For example, the results of the many decompositions were merged throughout the learning phase, the fundamental assumptions of probability may not always hold, which might result in inconsistencies. Additionally, rather than taking into account all of the model outputs when computing the specific probabilities, just two of them are at most taken into account. the proportion of positive to negative class in the severe groups is then noticeably out of balance after achieving the decomposition. This process may become implausible in the event of an already unbalanced database. A workaround is proposed to get around this restriction: one convolutional model can be trained concurrently and fed into several connected blocks, each of which solves a different binary classification subproblem. The training was carried out simultaneously and the unbalance to the learning data would be low severe. The likelihood $O_k = P(y > C_k|x) \in (0, 1)$ is represented by a sigmoid activation function at the $Q - 1$ completely integrated blocks’ outputs (0,1).

In this manner, categorization considerations are given to all model outputs.

$$y = \operatorname{argmin}_{1 < q < Q} d(0, C_q) \tag{4}$$

It is ensured that only the linking regions of each category are taken into account by using only the intersection of the two neighborhoods. The value of k would determine how large a region is taken into account.

$$f(e_{x,y}) = d(i_x, i_y) = \|i_x, i_y\|_2 \tag{5}$$

Figure 2 displays an illustration of the computed graph (V_q, E_q) . Finally, G_q can be used to create new synthetic samples: Random edge $E = (i_x, i_y) \in E_q$ is chosen in such a way to the section i_x and i_y to produce sample:

$$i' = (1 - \delta)i_x + \delta i_y \tag{6}$$

where δ is a random variable with a value between [0, 1]. The chosen edge E will determine the distribution from which δ is sampled.

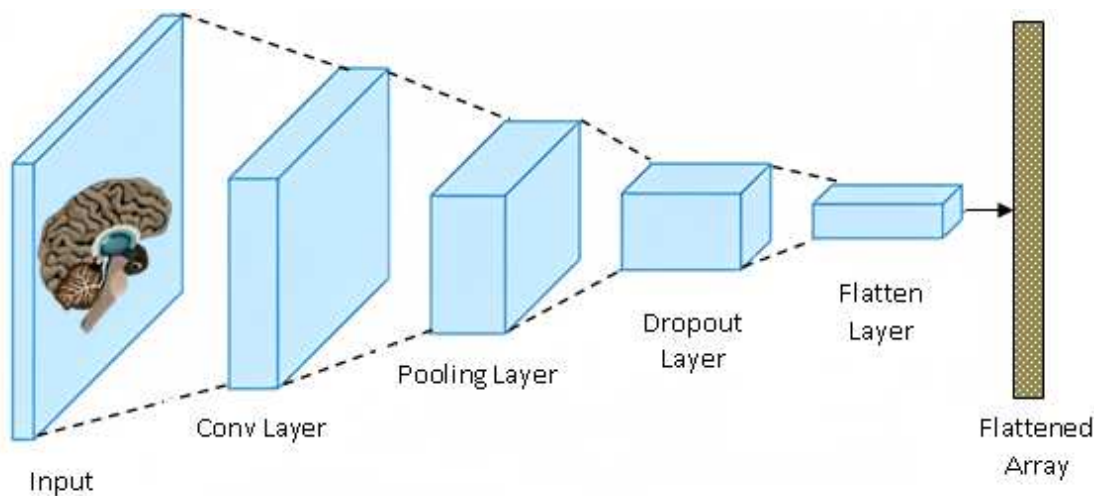


Fig. 1: 3D IFRCNN levels

For some datasets, including the one that will be the subject of this research, they believe the BD would make a good candidate for creating synthetic samples. ISP-OGO configurations (b) and (c) take advantage of the adaptability of the beta distribution, Although simply for comparison, configuration (a) mimics the initial gamma distribution. The same event occurs in both $\beta < 1$ and $\delta = 1$. In this method, it is possible to manage the likelihood of producing examples for the ICD favoring the production of examples to the increased class area relative to the neighboring category. Furthermore, Algorithm 1 specifies the specific process.

3.3 Experimental design

The entire dataset was subjected to a divided 5-fold cross-verification. A class distribution was preserved for each fold by stratifying the dataset into 5 equal-sized sections. A portion is used for testing for each stage, and the remainder is used as training data. The model selection procedure, which involves tuning the algorithm's hyperparameters, is carried out for each of these five phases in the first phase [30]. The characteristic combinations are ranked using the average MAE score for the three splits, and the optimum combination for each fold is then evaluated. The ideal parametric pairing is used in the 2nd stage for the final assessment once the hyperparameter selection phase was finished. For each of the data folds, the identical plan is repeated. Figure 3 provides a visual representation of this procedure.

Maximum - (↑) ;

Minimum - (↓);

ISP-OGO algorithm
Input: D- dataset; k: size of the neighborhood; n - iterations of class q; q - Augment class
Step 1: Set P D, q, n, k
{
Step 2: Graph constructed $G_q = (V_q, E_q)$
Step 3: Set $D' = \phi'$
Step 4: for x ranges from 1 to n
{
Step 4.1: Select random $e = (i_x, i_y)$ from E_q ,
Step 4.2: until $y_i = C_q \vee y_j = C_q$
Step 4.3: if $y_i = C_q \wedge y_j = C_q$ then
{
Step 4.4: Sample δ from distribution (uniform) $U(0, 1)$
}
else
{
Step 4.5: if $y_i \neq C_q$ then
{
Step 4.6: Assign $i_x, i_y = i_y, i_x$
Step 4.7: Sample δ from distribution (asymmetrical)
}
Step 5: Assign $i' = (1 - \delta)i_x + \delta i_y$
Step 6: $D' = D' \cup \{i'\}$
}
Step 7: return D'
}
}

N - No. of test specimens;

Q - No. of features;

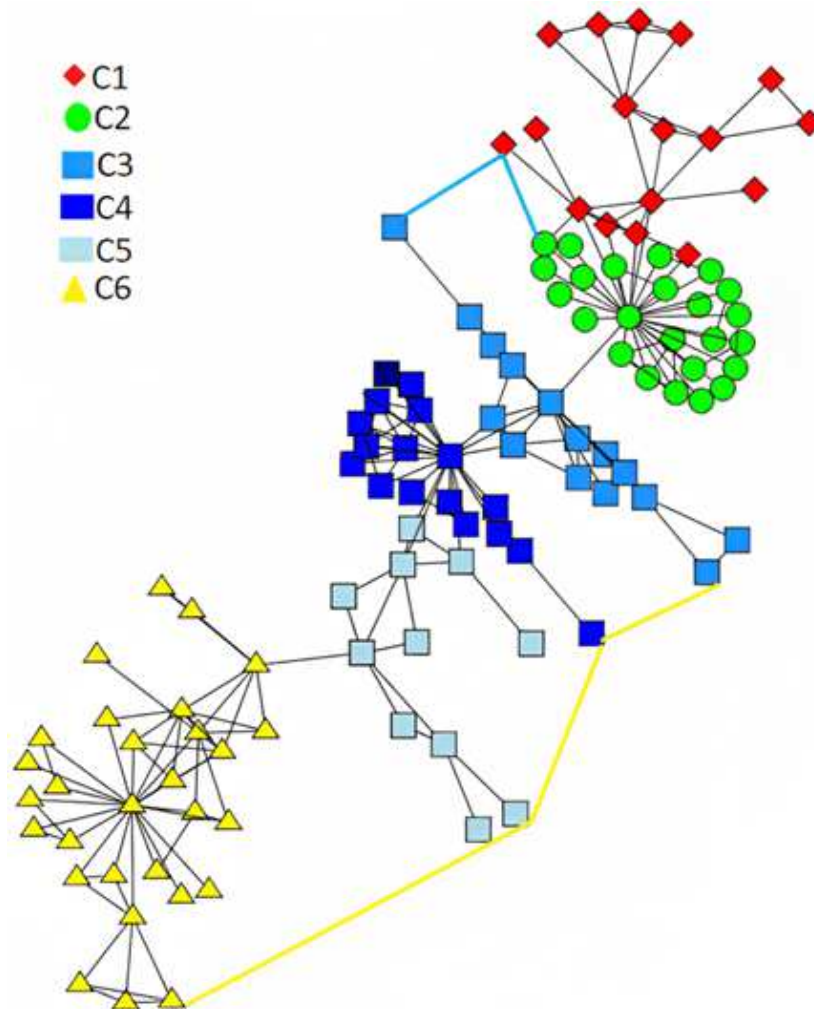


Fig. 2: An example of the ISP-OGO graph creation

$$CCR(\uparrow) : CCR = \frac{1}{N} \sum_{x=1}^N 1[\hat{y}_x = y_x] \quad (7)$$

Minimum sensitivity & geometric mean of susceptibility (\uparrow):

$$GMS = \sqrt[Q]{\prod_{q=1}^Q S_q} \quad (8)$$

$$MS = \min_{1 \leq q \leq Q} S_q \quad (9)$$

where per-class sensitivity (S_q) is:

$$S_q = \frac{\sum_{x=1}^N 1[y_x = \hat{y}_x = q]}{\sum_{x=1}^N 1[y_x = q]} \quad (10)$$

To assess the performance in these circumstances, class imbalance-sensitive measures MMAE, GMS, MS, MSp, AMAE and GMS were selected. The Receiver Operating Characteristic (ROC) curve (AUC) will then be computed depending on the output scores of the methods. This value is determined by obtaining as many curves as there are classes, with curve being binary One-vs-Rest (OvR) labeling. Finally, the Q curves are used to derive the average AUC. All Category 0 labels would be regarded as “negative class” or HC for this purpose, whereas the remaining labels (classes 1 through 3) would be regarded as “positive class” or PD. A confusion matrix could be obtained from this. The following metrics could be computed using the number of false negatives (FN), true negatives (TN), true positives (TP), false positives (FP), &:

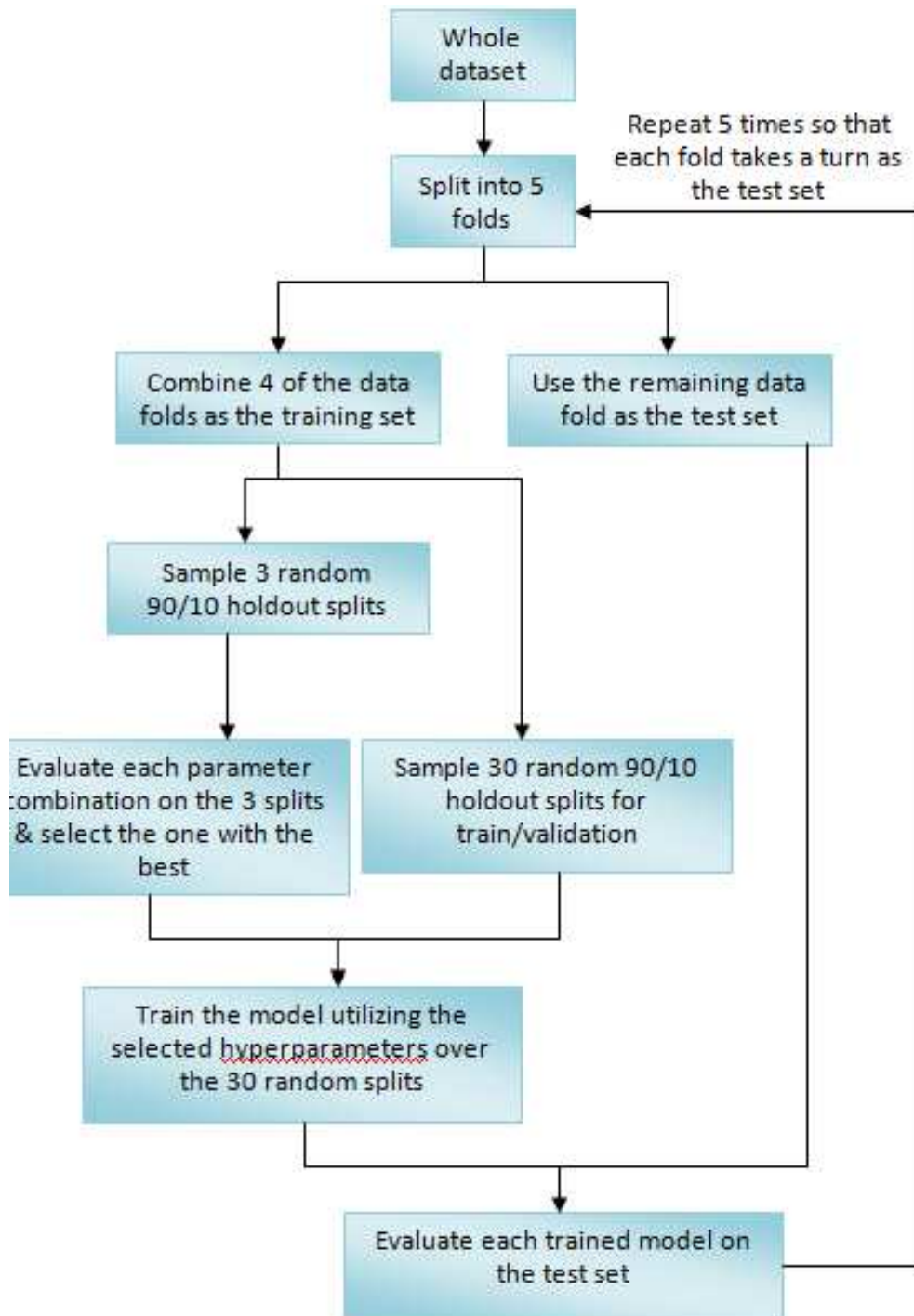


Fig. 3: The cross-verification method to verify the hyper parameters

Accuracy =

$$\frac{\text{True Positive} + \text{True Negative}}{\text{True Positive} + \text{True Negative} + \text{False Positive} + \text{False Negative}} \quad (11)$$

$$\text{Sensitivity} = \frac{\text{True Positive}}{\text{True Positive} + \text{False Negative}} \quad (12)$$

$$Specificity = \frac{True\ Negative}{True\ Negative + False\ Positive} \quad (13)$$

4 Results and discussions

A list of every result from the 150 iterations of the different strategies, depending on the various evaluation criteria described in the preceding section, is provided in Table 1. Figure 4 provides a graphic representation of the findings. These results demonstrate that, except CCR, for which the nominal, some configuration of ISP-OGO-β always outperforms all other classifiers in terms of average performance.

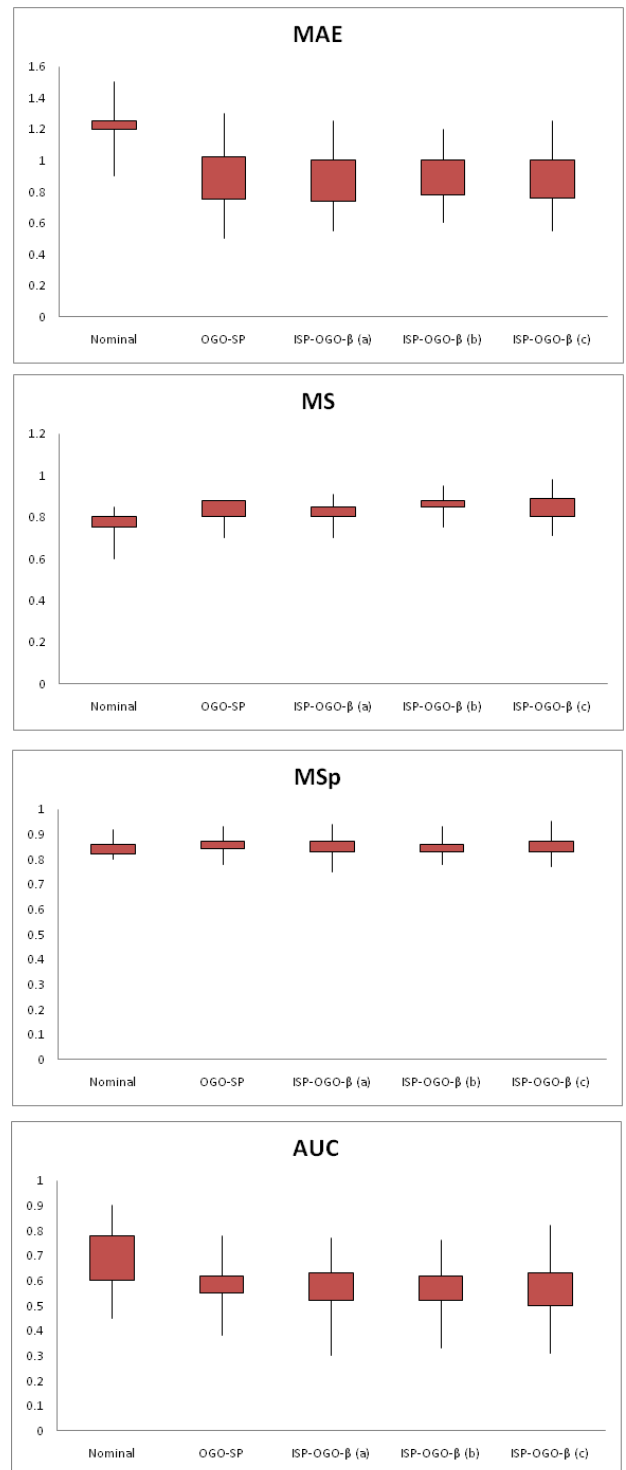
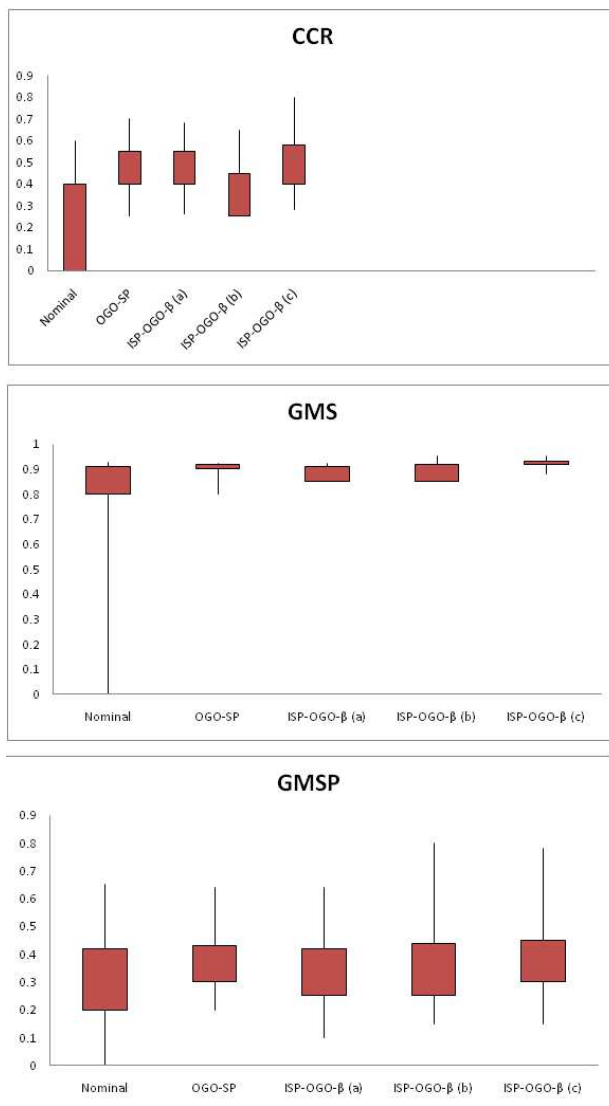


Table 1: The bolded findings represent the best mean results.

Method	CCR(↑)		GMS(↑)		MS(↑)		MSp(↑)		GMS(↑)		AUC(↑)	
	Mean	SD	Mean	SD	Mean	SD	Mean	SD	Mean	SD	Mean	SD
Nominal	0.7452	0.0413	0.1928	0.2016	0.0681	0.0775	0.7693	0.0571	0.8899	0.0180	0.8487	0.0349
OGO-SP	0.7125	0.0424	0.4258	0.1848	0.2427	0.1612	0.8277	0.0409	0.8982	0.0139	0.8589	0.03466
ISP-OGO-β (a)	0.7051	0.0489	0.4135	0.1893	0.2298	0.1576	0.8225	0.0408	0.8958	0.0151	0.8554	0.0387
ISP-OGO-β(b)	0.7110	0.0646	0.4241	0.1735	0.2236	0.1477	0.8295	0.0602	0.8979	0.0231	0.8568	0.0333
ISP-OGO-β(c)	0.7256	0.0425	0.4410	0.1831	0.2462	0.1453	0.8315	0.0513	0.9009	0.0172	0.8599	0.0368

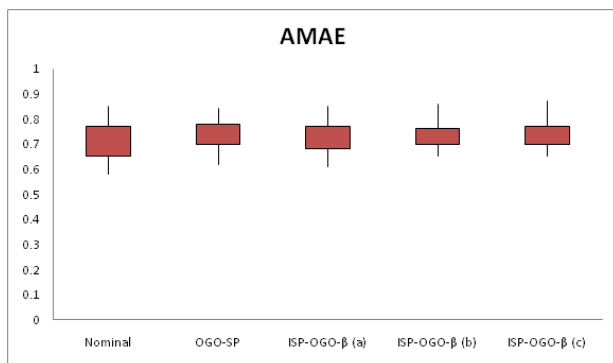


Fig. 4: Graph showing the experimentation findings

The nominal methodology is outperformed by both ordinal approaches. The appropriate ROCs are displayed in Figure 5 for each class of the problem. An advanced minority category, particularly for category 1, which has the fewest samples, both ordinal approaches show a definite benefit. To find significant differences between the metrics, they used a WSR evaluation. Due to the characteristics' shared sample; this test version was utilized to evaluate the performance of the classifiers. OGO-SP-β, the best-performing internal approach, and purely nominal methodology were compared. The test was additionally utilized to compare the ISP-OGO-β ordinal approach with the ISP-OGO-β ordinal method, which had the best performance.

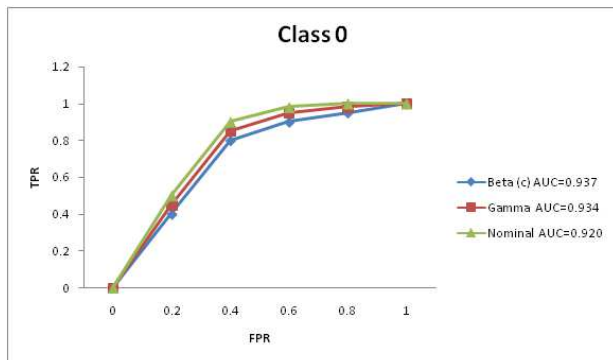
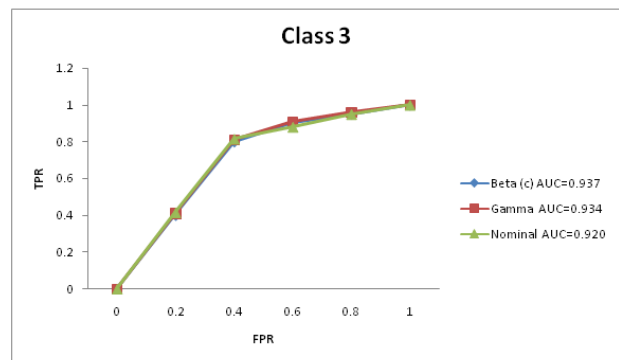
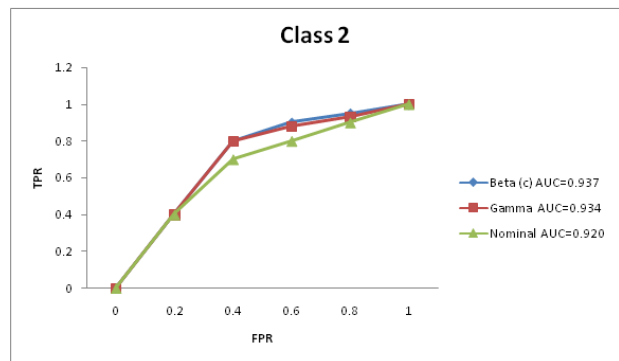
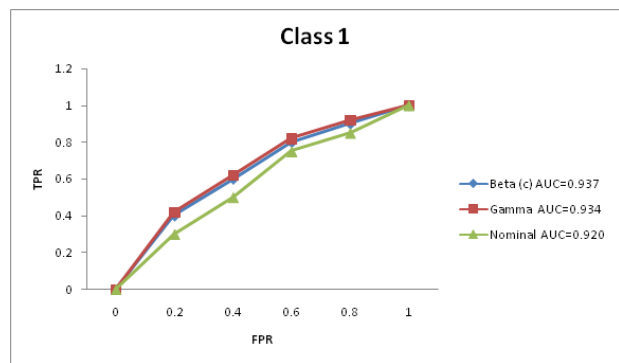


Fig. 5: The ROC values derived for the 4 categories

Table 2 contains the results for the binary metrics. The outcomes are evaluated in comparison to the following works: Notice that the problem under consideration in

Table 2: The binary metrics produced by the proposed methods

Method	Type	Data	Accuracy	Sensitivity	Specificity
Nominal	A	I	88.63	78.53	84.85
OGO-SP	A	I	88.32	87.56	88.65
ISP-OGO- β (a)	A	I	87.95	87.68	88.10
ISP-OGO- β (b)	A	I	88.15	88.11	88.17
ISP-OGO- β (c)	A	I	89.20	87.22	90.39

these works is distinct since the many positive labeling alternatives are not distinguished, considerably lowering the complexity. Although if the offered approaches are more informative and the different parameters and datasets are different, they could still claim that the performance attained by the various ideas is competitive, especially when seeking to strike an equilibrium among all three binary measures. In other words, the extra data made available by the proposed multiclass category was obtained at the expense of decreased efficiency in the binary operation.

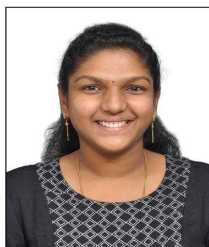
5 Conclusion

Researchers are demonstrated experimentally that the use of ordinal data could enhance the effectiveness of a challenging task, the evaluation of changes in brain movement of PD. A data augmentation optimization aim, and model design, approach are some of the factors that contribute to this exploitation. This broadens the present selection of model, a fully 3D IFRCNN-that may make use of ordinal information. This approach can reduce the issue of class unbalance by enhancing ordinal effectiveness indicators. A method can be used to improve ordinal categorization methods that already exist and have the same issue, which is widespread in the medical industry. Furthermore, the efficiency of nominal & ordinal metrics is enhanced by the proposed ISP-OGO- β ordinal augmentation method in comparison to the original OGO-SP. The evaluation of expert predictions and other ML approaches demonstrates good performance from the perspective of the more traditional binary diagnosis.

References

- [1] A. Surguchov, Biomarkers in Parkinson's disease. *Neurodegenerative diseases biomarkers: Towards translating research to clinical practice*, 155-180, (2022).
- [2] Q. Hassan, S.Li, C. Ferrag, and K. Kerman, Electrochemical biosensors for the detection and study of α -synuclein related to Parkinson's disease-a review, *Analytical chimica acta*, 1089, 32-39. (2019).
- [3] L. Parnetti, L. Gaetani, P. Eusebi, S. Paciotti, O.Hansson, O. El-Agnaf, and P. Calabresi, CSF and blood biomarkers for Parkinson's disease, *The Lancet Neurology*, **18**(6), 573-586, (2019).
- [4] B. Shen, Y. Lin, C. Bi, S. Zhou, Z. Bai, G. Zheng, and J. Zhou, Translational informatics for Parkinson's disease: from big biomedical data to small actionable alterations, *Genomics, Proteomics & Bioinformatics*, **17**(4), 415-429, (2019).
- [5] A. Gialluisi, M. G. Reccia, N. Modugno, T. Nutile, A. Lombardi, L.G. Di Giovannantonio, and T. Esposito, Identification of sixteen novel candidate genes for late-onset Parkinson's disease, *Molecular neurodegeneration*, **16**(1), 1-18, (2021).
- [6] T.R. Yamasaki, B.B. Holmes, J.L. Furman, D.D. Dhavale, B.W. Su, E.S. Song, and M.I. Diamond, Parkinson's disease and multiple system atrophy have distinct α -synuclein seed characteristics, *Journal of Biological Chemistry*, **294**(3), 1045-1058, (2019).
- [7] E.M. Cilento, L. Jin, T. Stewart, M. Shi, L. Sheng, and J. Zhang, Mass spectrometry: A platform for biomarker discovery and validation for Alzheimer's and Parkinson's diseases, *Journal of neurochemistry*, **151**(4), 397-416, (2019).
- [8] R.M. Sadek, S.A. Mohammed, A.R.K. Abunbehan, A. K. H. A., Ghattas, M.R. Badawi, M.N. Mortaja, and S.S. Abu-Naser, Parkinson's disease prediction using artificial neural network, (2019).
- [9] E. Tadayon, A. Pascual-Leone, D. Press, E. Santarnecchi, and Alzheimer's Disease Neuroimaging Initiative, Choroid plexus volume is associated with levels of CSF proteins: relevance for Alzheimer's and Parkinson's disease, *Neurobiology of aging*, **89**, 108-117, (2020).
- [10] X. Teng, S. Mao, H. Wu, Q. Shao, J. Zu, W. Zhang, and C. Xu, The relationship between serum neurofilament light chain and glial fibrillary acidic protein with the REM sleep behavior disorder subtype of Parkinson's disease, *Journal of Neurochemistry*, (2023).
- [11] A. Picca, F. Guerra, R. Calvani, R. Romano, H.J. Coelho-Júnior, C. Bucci, and E. Marzetti, Mitochondrial dysfunction, protein misfolding and neuroinflammation in Parkinson's disease: Roads to biomarker discovery, *Biomolecules*, **11**(10), 1508, (2021).
- [12] B.C. Uzuegbunam, D. Librizzi, and B. HooshyarYousefi, PET radiopharmaceuticals for Alzheimer's disease and Parkinson's disease diagnosis, the current and future landscape, *Molecules*, **25**(4), 977, (2020).
- [13] M. Repici, and F. Giorgini, DJ-1 in Parkinson's disease: clinical insights and therapeutic perspectives. *Journal of clinical medicine*, **8**(9), 1377, (2019).
- [14] N. S, R. V. D and R. J, *COVID-19 Prediction using LSTM*, 2022 6th International Conference on Intelligent Computing and Control Systems (ICICCS), Madurai, India, 254-259, (2022).
- [15] C.O. Sakar, G. Serbes, A. Gunduz, H. C. Tunc, H. Nizam, B.E. Sakar, and H. Apaydin, A comparative analysis of speech signal processing algorithms for Parkinson's disease classification and the use of the tunable Q-factor wavelet transform, *Applied Soft Computing*, **74**, 255-263, (2019).
- [16] L.M. Oliveira, T. Gasser, R. Edwards, M. Zweckstetter, R. Melki, L. Stefanis, and T.F. Outeiro, Alpha-synuclein research: Defining strategic moves in the battle against Parkinson's disease, *npj Parkinson's Disease*, **7** (1), 65, (2021).
- [17] J. Peng, J. Guan, and X. Shang, Predicting Parkinson's disease genes based on node2vec and autoencoder, *Frontiers in genetics*, **10**, 226, (2019).

- [18] L. Gao, W. Wang, X. Wang, F. Yang, L. Xie, J. Shen, and S.Q. Yao, Fluorescent probes for bioimaging of potential biomarkers in Parkinson's disease, *Chemical Society Reviews*, **50**(2), 1219-1250, (2021).
- [19] S. Mao, X. Teng, Z. Li, J. Zu, T. Zhang, C. Xu, and G. Cui, Association of serum neurofilament light chain and glial fibrillary acidic protein levels with cognitive decline in Parkinson's disease. *Brain Research*, 1805, 148271, (2023).
- [20] S. Zhao, H. Chi, Q. Yang, S. Chen, C. Wu, G. Lai, and P. Lu., Identification and validation of neurotrophic factor-related gene signatures in glioblastoma and Parkinson's disease. *Frontiers in Immunology*, **14**, (2023).
- [21] Q. Lv, Z. Wang, Z. Zhong, and W. Huang, Role of long noncoding RNAs in Parkinson's disease: putative biomarkers and therapeutic targets, *Parkinson's Disease*, (2020).
- [22] L. Seguella, G. Sarnelli, and G. Esposito, Leaky gut, dysbiosis, and enteric glia activation: the trilogy behind the intestinal origin of Parkinson's disease, *Neural Regeneration Research*, **15**(6), 1037, (2020).
- [23] E.W. Lim, D. Aarsland, D. Ffytche, R.N. Taddei, D.J. van Wamelen, Y.M. Wan, and Kings Parcogroup MDS Nonmotor study group, Amyloid- β and Parkinson's disease, *Journal of Neurology*, **266**, 2605-2619, (2019).
- [24] M.T. Mackmull, L. Nagel, F.Sesterhenn, J. Muntel, J. Grossbach, P. Stalder, and P. Picotti, Global, in situ analysis of the structural proteome in individuals with Parkinson's disease to identify a new class of biomarker, *Nature structural & molecular biology*, **29**(10), 978-989, (2022).
- [25] E.H. Kwon, S. Tennagels, R. Gold, K. Gerwert, L. Beyer, and L. Tonges, Update on CSF biomarkers in Parkinson's disease, *Biomolecules*, **12**(2), 329, (2022).
- [26] P. Arora, A. Mishra, and A. Malhi, Machine learning Ensemble for the Parkinson's disease using protein sequences, *Multimedia Tools and Applications*, **81**(22), 32215-32242, (2022).
- [27] A. Naha, S. Banerjee, R. Debroy, S. Basu, G. Ashok, P. Priyamvada, and S. Ramaiah, Network metrics, structural dynamics and density functional theory calculations identified a novel Ursodeoxycholic Acid derivative against therapeutic target Parkin for Parkinson's disease, *Computational and Structural Biotechnology Journal*, **20**, 4271-4287, (2022).
- [28] I.S. Nila, D.M. Sumsuzzman, Z.A. Khan, J.H. Jung, A.S. Kazema, S.J. Kim, and Y. Hong, Identification of exosomal biomarkers and its optimal isolation and detection method for the diagnosis of Parkinson's disease: A systematic review and meta-analysis, *Ageing Research Reviews*, 101764, (2022).
- [29] X. Cao, F. Yang, J. Zheng, X. Wang, and Q. Huang, Aberrant structure MRI in Parkinson's disease and comorbidity with depression based on multinomial tensor regression analysis, *Journal of Personalized Medicine*, **12**(1), 89, (2022).
- [30] I. Berdowska, M. Matusiewicz, and Krzystek-Korpaczka, HDL Accessory Proteins in Parkinson's Disease-Focusing on Clusterin (Apolipoprotein J) in Regard to Its Involvement in Pathology and Diagnostics-A Review, *Antioxidants*, **11**(3), 524, (2022).
- [31] X. Teng, S. Mao, H. Wu, Q. Shao, J. Zu, W. Zhang, and C. Xu, The relationship between serum neurofilament light chain and glial fibrillary acidic protein with the REM sleep behavior disorder subtype of Parkinson's disease, *Journal of Neurochemistry*, (2023).



Caroline El Fiorenza J is a research scholar in the Department of Computer Science and Engineering of SRM Institute of Science and Technology, Chennai. She has overall experience of 8+ years in the field Academic & Administration. She has been part of SRM group over 7 years and has served various academic and administrative roles. She currently holds the position of Senior Assistant Professor. She is an Alumina of SRM University, Kattankulathur and Vellore Institute of Technology, Vellore. She has authored and co-authored research publications. She has experience in Computer Science, with emphasis on Algorithms and research interest in Data Mining, Deep Learning and Artificial Intelligence.



V. Sellam has overall experience of 11+ years in the field of Information Technology, Projects and in Academic & Administration. She has been part of SRM group over 8+ years and has served various academic and administrative roles. With Eight years of academic contribution and 3 years of industrial experience currently holds the position of Senior Assistant Professor. She has obtained her Doctorate in Computer Science and Engineering from SRM Institute of Science and Technology, Chennai and Masters from Annamalai University. She has authored and co-authored research publications and books as her contributions. Her research alignment is broadly in the areas of Agricultural Data Mining, Speech processing